Continuation-Based Quasi-Steady-State Analysis

Qin Wang, *Member, IEEE*, Hwachang Song, *Member, IEEE*, and Venkataramana Ajjarapu, *Senior Member, IEEE*

***Abstract*—This paper presents continuation-based quasi-steady-state (CQSS) analysis to approximate the long-term evolution by tracing successive equilibrium points. Applying the parameterized continuation technique to QSS simulation can provide good convergence when the system approaches the bifurcation points. Parameterization of the load exponents through continuation method makes it possible to simulate dynamic load recovery models in the system without numerical integration. The tap dynamics are also included in the CQSS analysis. The simulation results with the modified WECC 179-bus system are described in order to demonstrate the overall methodology.**

***Index Terms*—Continuation method, load restoration, long-term voltage instability, quasi-steady-state (QSS) simulation, voltage stability.**

I. Introduction

VOLTAGE stability has become a major concern for the secure operation of worldwide systems. Voltage stability problems can be classified in different time scales [1]–[3]. Recently, Kundar *et al.* [4] standardized the voltage stability definition in the short-term and long-term time scales. This paper addresses the voltage instability in long-term time scale, and proposes a robust simulation tool for analyzing the system's voltage stability in the long-term time scale.

To demonstrate the methodology, two scenarios are first defined as follows.

- *Scenario One*: The post-contingency long-term load characteristic intersects the system PV curve (see Fig. 1).
- *Scenario Two*: The post-contingency long-term load characteristic does not intersect the system PV curve (see Fig. 2).

In *Scenario One* (see Fig. 1), the short-term load characteristic is fully restored to the long-term load characteristic. At first, the system is at its pre-contingency operating point A. Due to the short-term load characteristic, the system jumps to A' just after the contingency. Each point on the post-contingency PV curve is the short-term equilibrium before the complete restoration (B) and the long-term equilibrium afterwards. Once the restoration is fully achieved, the load is increased to dominate the system's evolution. In Fig. 1, the long-term saddle-node bifurcation (SNB) point C needs to be identified during the equilibrium tracing in order to obtain the information of how much active power margin the system has from point B.

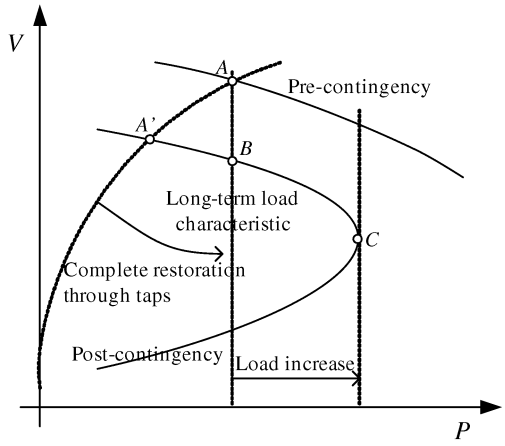

Fig. 1. Simulation for *Scenario One*.

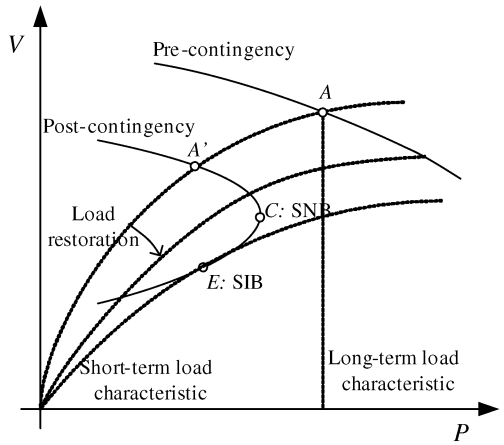

Fig. 2. Simulation for *Scenario Two*.

In *Scenario Two* (see Fig. 2), if the contingency is severe and no long-term equilibrium exists after such a contingency, then the system will be unsolvable with respect to long-term load characteristic. Load dynamics drive the system from one equilibrium of the fast dynamics to another by changing the short-term load characteristic. Under this condition, each point on the post-contingent PV curve is a short-term equilibrium. The system finally reaches the singularity-induced bifurcation (SIB) [8] point E in Fig. 2 and may experience voltage collapse. During this process, the system crosses the long-term critical point C where the SNB results in the long-term time scale. The post-contingency PV curve is very useful when the corrective control actions, such as load shedding, are implemented to stabilize an unstable power system, by directing the system's trajectory onto a new stable equilibrium point. From

Manuscript received October 17, 2002; revised April 4, 2005. Paper no. TPWRS-00477-2002.

Q. Wang is with EMC Corporation, Hopkinton, MA 01748 USA (e-mail: qwanghz@yahoo.com).

H. Song is with the School of Electronic and Information Engineering, Kunsan National University, Jeonbuk 573-701, Korea (e-mail: hcsong@kunsan.ac.kr).

V. Ajjarapu is with the Department of Electrical Engineering and Computer Engineering, Iowa State University, Ames, IA 50011 USA (e-mail: vajjarap@iastate.edu).

Digital Object Identifier 10.1109/TPWRS.2005.860936

the long-term point of view, it is required to decrease a certain amount of load below the value corresponding to SNB point in order to create a new long-term equilibrium. The difference of active loads between A and C can be a good estimate for determining the adequate amount of load shedding. From the short-term point of view, the new intersection of the short-term load characteristic due to load shedding and the post-contingency PV curve should be located in the region of attraction of the new long-term equilibrium. Also the corrective control should be carried out before the post-contingency system reaches the SIB point E.

For the above scenarios, a continuation-based quasi-steady-state (CQSS) simulation will be applied to trace the system's trajectories. QSS analysis has been widely used to speed up the voltage stability calculation in the long-term time scale [2]–[5], [8]. The major long-term dynamic phenomena that have been taken into account in this paper are voltage or load restoration by on-load tap changer transformers (OLTCs) and thermostatic load restoration.

Van Cutsem proposes the general idea of QSS analysis in [5]. It offers a good compromise between the efficiency of power-flow-type methods and the modeling advantage of full time-domain methods. However, the original QSS simulation encounters numerical difficulties when the system approaches point E. This SIB in *Scenario Two* cannot be readily identified since the Jacobian matrix [5] for solving short-term equilibrium points becomes singular near SIB.

In order to overcome this singularity problem, the continuation method can be applied to solve the system equations. In addition, the continuation approach can provide a more convenient way to consider load restoration and load increase in a coordinated way in *Scenario One*. Moreover, QSS analysis incorporates the thermostatic load self-restoration, which is represented by the differential equations in the long-term time scale. The power consumed by the load at any time depends upon the instantaneous value of a state variable representing load restoration [11]. During QSS simulation, the equilibrium of the system's fast dynamics should be recalculated after the integration of the load state variable, which would increase the computational cost.

References [6] and [11] further solve the load restoration analytically for a step change in voltage. Based on this derivation, another way to consider the load restoration in the CQSS simulation is proposed here [12]. It eliminates the need for numerical integration in the simulation and simplifies the whole tracing procedure. By appropriately predicting the continuation parameter, this method is a very close approximation to the differential representation of the load restoration. It will also avoids the computation difficulty around the SIB point.

In this paper, with different continuation parameters, the CQSS simulation identifies voltage collapse during the equilibrium tracing. We take into account both the load increase and the OLTC dynamics, as well as the thermostatic load self-restoration. The above approach leads to integration of various aspects discussed in [2], [5], [6], and [9]–[11].

The major contributions of this paper can be explained as follows. First, due to the continuation method, CQSS is numerically well conditioned, and the singularity checking of Jacobian matrix such as calculating matrix determinant can be eliminated. Second, parameterization of the load exponent provides a new way to simulate the load restoration in QSS analysis; in addition, this removes numerical integration. Third, the combined effects of OLTCs and load change on voltage stability can be taken into account.

This paper is organized as follows. Section II briefly describes a general modeling setup that includes generic load model and the OLTC control logic. Then Section III introduces the methodology for equilibrium tracing in the long-term time scale by using the CQSS simulation. Section IV further provides details regarding parameterization needed for CQSS simulation for load exponent in load restoration in *Scenario One* as well as in *Scenario Two*. Section V associates the load change (λ) or the load exponent (α) with the time. Numerical results of the modified WECC system are described in Section VI.

II. Problem Formulation

A general modeling relevant to voltage stability in different time scales is described from the following set of equations [3] (this includes differential, algebraic, and discrete sets of equations):

$$\frac{d}{dt}x = f(x, y, z_D, z_C, \lambda) \tag{1}$$

$$0 = g(x, y, z_D, z_C, \lambda) \tag{2}$$

$$z_D(k^+) = h_D(x(k^-), y(k^-), z_D(k^-), z_C(k^-), \lambda(k)) \tag{3}$$

$$\frac{d}{dt}z_C = h_C(x, y, z_D, z_C, \lambda) \tag{4}$$

where $f(\cdot)$ in (1) describes the dynamics of synchronous machines, the excitation systems, the prime mover, and speed governors, and $g(\cdot)$ in (2) represents the system network functions. Equations (1) and (2) involve the transient state variables x and algebraic variables y, respectively. The variable y usually relates to network bus voltage magnitudes and angles. The long-term dynamics are captured by discrete and/or continuous time variables in (3) and (4), respectively. z_D relates to discrete controls such as tap changers. z_C represents continuous load recovery dynamics. Finally, λ in (1)–(4) denotes changes in demand and the corresponding generation rescheduling. For QSS simulation, (1) will be replaced by its equilibrium equation.

In *Scenario One*, in order to explore the influence of OLTCs on voltage stability, z_C is not addressed to simplify the simulation process. In *Scenario Two*, however, we consider both tap as well z_C. A new approach is adopted to consider the load restoration. The transition times k are dictated by built-in delays or sampling periods of these devices and controls.

Load model plays an important role in voltage stability analysis. Generally, the power consumed by the transient generic load is given by

$$P_l = P_t = P_{l0}\left[z_P + \left(\frac{V}{V_0}\right)^{\alpha_T}\right] \tag{5a}$$

$$Q_l = Q_t = Q_{l0}\left[z_Q + \left(\frac{V}{V_0}\right)^{\beta_T}\right] \tag{5b}$$

where z_P and z_Q [correspond to z_c in (4)] are internal state variables associated with generic load dynamics. They are depicted in the following equations [2], [5]:

$$T_P \frac{d}{dt} z_P = -z_P + \left(\frac{V}{V_0}\right)^{\alpha_S} - \left(\frac{V}{V_0}\right)^{\alpha_T} \tag{6a}$$

$$T_Q \frac{d}{dt} z_Q = -z_Q + \left(\frac{V}{V_0}\right)^{\beta_S} - \left(\frac{V}{V_0}\right)^{\beta_T}. \tag{6b}$$

The steady-state load characteristics are

$$P_l = P_s = P_{l0}\left(\frac{V}{V_0}\right)^{\alpha_S} \tag{7a}$$

$$Q_l = Q_s = Q_{l0}\left(\frac{V}{V_0}\right)^{\beta_S}. \tag{7b}$$

Usually, the transient load exponents α_T and β_T are larger than the steady-state ones α_S and β_S. $P_{\rm lo}$ and $Q_{\rm lo}$ are the powers absorbed by the load at the nominal voltage V_0.

The tap-changing logic at time instant t_k [5] is given as follows:

$$r_{k+1} = \begin{cases} r_k + \Delta r, & \text{if } V_2 > V_2^0 + d \quad \text{and} \quad r_k < r_{\max} \\ r_k - \Delta r, & \text{if } V_2 < V_2^0 - d \quad \text{and} \quad r_k > r_{\min} \\ r_k, & \text{otherwise} \end{cases}$$

where V_2 is the controlled voltage after OLTC, V_2^0 is the reference voltage, d is half the OLTC dead-band, and $r_{\max}$ and $r_{\min}$ are the upper and lower tap limits.

III. Implementation of the Continuation Method

As mentioned before, QSS simulation has been widely used to speed up the log-term voltage stability calculations, which filters out the short-term transients. It deals with the long-term subsystem of the DAEs based on the assumption that the transient subsystem is infinitely fast and can be replaced by its equilibrium equations. Therefore, in the QSS analysis, the short-term dynamics dx/dt in (1) are replaced with 0 to obtain equilibrium points

$$0 = f(x, y, z_D, z_C, \lambda). \tag{8}$$

CQSS solves both (8) and (2), with changing λ, z_D, and z_c. The change of z_c in (4) is realized through load exponents (α/β). In CQSS, α or β is parameterized to simulate the load restoration. When α is chosen as continuation parameter, the system undergoes continuous evolution directed by the change of the aggregate load components and types. This parameterization avoids the integration of z_c in (4) and relates P_l and Q_l in terms of $\alpha(t)/\beta(t)$. The derivation is explained in Section IV.

The simplified QSS simulation methodology is outlined in Fig. 3. Point A is an equilibrium before the disturbance. Point A' is an equilibrium of these equations after the disturbance. The continuous change from A' to B results from the evolution of λ or α. The transition from B to B' is from the discrete change of z_D. If you considered the variation of λ (or α), then the continuation method traces the equilibrium defined by (8) and (2) for a fixed z_D. It is seen that x/y and z_D variables are separately considered. The Jacobian matrix only involves the derivatives of f/g with respect to x/y.

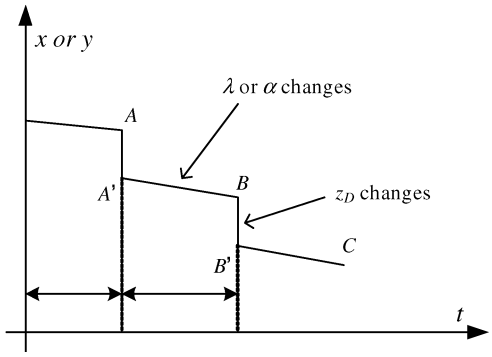

Fig. 3. Time evolution of an x and y component [5].

In CQSS, the same procedure of the original QSS is realized using the predictor and corrector in continuation method. The continuation method traces the equilibrium for changing λ (or α). It involves a prediction (9) and a correction (10) to find the equilibrium point

$$-\begin{pmatrix} f_x & f_y & f_\lambda \\ g_x & g_y & g_\lambda \\ & e_k^T & \end{pmatrix}\begin{pmatrix} dx \\ dy \\ d\lambda \end{pmatrix} = \begin{pmatrix} 0 \\ 0 \\ \pm 1 \end{pmatrix} \tag{9}$$

$$-\begin{pmatrix} f_x & f_y & f_\lambda \\ g_x & g_y & g_\lambda \\ & e_k^T & \end{pmatrix}\begin{pmatrix} \Delta x \\ \Delta y \\ \Delta \lambda \end{pmatrix} = \begin{pmatrix} f \\ g \\ 0 \end{pmatrix} \tag{10}$$

where $(dx\ dy\ d\lambda)^T$ is the tangent vector. e_k^T is a row unit vector with all the elements equal to zero except for the kth one. In (9) and (10), f_λ and g_λ are not null vectors, even at the base case, and e_k^T is selected to indicate continuation parameter. The singularity of the augmented Jacobian matrix can be avoided by the appropriate selection of continuation parameter. In order to locate the bifurcation point, first in the prediction, a relatively large step size is used to trace the system's long-term equilibrium until a negative $d\lambda$ is detected at some point, which is located on the lower part of the PV curve. Then we change the tracing direction and continue the simulation with a smaller step size up to the bifurcation point, where null $d\lambda$ could be easily detected.

If null $d\lambda$ or $d\alpha$ is detected in the predictor step at some time step, (9) will reduce to

$$\underbrace{\begin{pmatrix} f_x & f_y \\ g_x & g_y \end{pmatrix}}_{J_{xy}}\begin{pmatrix} dx \\ dy \end{pmatrix} = J_{xy}\begin{pmatrix} dx \\ dy \end{pmatrix} = \begin{pmatrix} 0 \\ 0 \end{pmatrix}. \tag{11}$$

In (11), $(dx\ dy)^T$ is not a null vector since one component of it should be ± 1. Then (11) implies the singularity of J_{xy}. From the detailed analysis of the system's total Jacobian and reduced system state matrices in the different time scales, we know that the singularity identified by null $d\lambda$ or $d\alpha$ corresponds to the SIB point.

When the system approaches the SIB point of long-term dynamics, J_{xy} becomes ill-conditioned. This may result in longer solution time or a divergent solution before the Jacobian actually becomes singular. The continuation method is well suited for dealing with such a problem. It remains feasible over the entire solution path, even at the critical point, by choosing an

appropriate continuation parameter. Mathematically, the continuation parameter corresponds to the state variable that has the largest tangent vector component. More simply put, this is the state variable that has the greatest rate of change near the given solution. In power systems, the load parameter λ is probably the best choice when starting from the base case. This is especially true if the base case is characterized by normal or light loading. Under such conditions, the voltage magnitudes and angles remain fairly constant under load change. Once the load is increased by a number of continuous steps and the solution path approaches the SNB point, voltage magnitudes and angles will likely experience significant change. At this point, λ is a poor choice of continuation parameter since it may change only a very small amount compared to other state variables. Therefore, the selection of continuation parameter should be re-evaluated at each step. For instance, the voltage magnitude at some particular bus could be changed by small amounts, and the solution could be found for each given value of the voltage. Here, the load parameter would be free to take on any value it needed to satisfy the system equations.

The predictor step can provide several advantages, including valuable sensitivity information as well as reduction of iterations in the corrector step. Calculating the tangent vector in the predictor corresponds to one iteration of the Newton–Raphson (N-R) method in the corrector. In our experience, however, it is certain that prediction of the next solution using the tangent vector is effective in the reduction of N-R iterations in the corrector.

IV. Parameterization of α for Scenario Two

This section describes an approach to deal with the load restoration procedure described by differential equations (6a) and (6b), for *Scenario Two*.

Assuming any reference voltage V_0, the sensitivities of real power and reactive power with respect to voltage can be obtained as

$$\frac{dP/P_{l0}}{dV/V_0} = \alpha \tag{12a}$$

$$\frac{dQ/Q_{l0}}{dV/V_0} = \beta. \tag{12b}$$

Thus, the normalized sensitivities of real and reactive load power with respect to voltage are equal to the corresponding load exponents by using the exponential load model. It means the sensitivity of the load power to voltage varies continuously during the load restoration procedure. In some sense, the load obeys an exponential model that changes from the transient α_T to the steady-state α_S exponent.

If the dynamics of the load restoration are considered completely, the differential equation related to the load state variable should be analyzed in the whole system DAEs. However, compared to the OLTC action, thermostatic load restoration belongs to "slow dynamics," even though they are treated in the same time scale. We assume that load dynamics still stay in a time-dependent exponential state at each short-term equilibrium. The load restoration is a procedure in which sensitivities change with the time. Therefore, the following equations are proposed to describe the load restoration:

$$P_l = P_{l0}\left(\frac{V}{V_0}\right)^{\alpha(t)} \tag{13}$$

$$Q_l = Q_{l0}\left(\frac{V}{V_0}\right)^{\beta(t)} \tag{14}$$

where $\alpha_S \le \alpha(t) \le \alpha_T$, and $\beta_S \le \beta(t) \le \beta_T$.

Next, we will show how to relate (13) and (14) to the original differential equations of the generic load restoration. In [6] and [11], for the additive load model

$$T_P\frac{d}{dt}P_l + P_l = P_S(V) + T_P\frac{d}{dt}(P_T(V)). \tag{15}$$

This was converted to the following form by introducing the state variable in [6]:

$$\frac{d}{dt}x_P = -\frac{1}{T_P}x_P + N(V) \tag{16}$$

$$x_P = T_P(P_l - P_T(V)) \tag{17}$$

$$N(V) = P_S(V) - P_T(V) \tag{18}$$

where $P_S(V) = P_{l0}(V/V_0)^{\alpha_S}$, and $P_T(V) = P_{l0}(V/V_0)^{\alpha_T}$ for the exponential load model. By setting $x_P = T_P P_{l0} z_P$, we can transform (16) to (6a) and (17) to (5a).

In [11], the above set of equations is solved analytically. The expression for x_P, which is the response to the voltage step from V_0 to V_1, can be obtained as follows:

$$x_P = T_P N(V_1) + T_P[N(V_0) - N(V_1)]e^{\frac{-(t-t_0)}{T_P}}. \tag{19}$$

Then from (17) and (18)

$$P_l(t) = P_S(V_1) + [P_S(V_0) - P_T(V_0) - P_S(V_1) + P_T(V_1)]e^{\frac{-(t-t_0)}{T_P}}, \quad t > t_0. \tag{20}$$

Assuming that $P_S = P_{l0}$ and (13) and (20), the following equation can be obtained to predict $\alpha(t)$ at each time step in the CQSS simulation:

$$\alpha(t) = \log_{(\frac{V}{V_0})}\left\{1 + \left[\left(\frac{V}{V_0}\right)^{\alpha_T} - 1\right]e^{\frac{-(t-t_0)}{T_P}}\right\}, t > t_0. \tag{21}$$

Based on the above derivation, we can see that the continuation parameter establishes a link between the load self-restoration and the QSS simulation conveniently.

Generally, the total system load level is chosen as the system parameter since the system can be fully recovered to the pre-contingency level in *Scenario One*. However, for *Scenario Two*, the total system power load cannot be completely restored to the pre-contingency level. During the load restoration process, the system will reach the SIB. Hence, it is not appropriate to increase the system load level. In order to simulate the load restoration, α and/or β will be chosen as the system parameter. Parameterization of the load exponent indicates that the system undergoes continuous evolution directed by the change of the aggregate load components and types.

In QSS simulation for *Scenario Two*, there can be many thermostatic loads and hence many load exponents in the system. Even though all the dynamic load have the same α_T,

and $\alpha_S, \alpha(t)$s can be different, depending on bus voltage, V_0 and T_P. At each time step, thus, CQSS needs to select one of them as the system parameter. For this purpose, it calculates $d\alpha/dt$ of each dynamic load, which can be derived from (21), and chooses one (α_{select}) with the largest $d\alpha/dt$ as the system parameter. In *Scenario Two*, therefore, the augmented Jacobian used in predictor and corrector can be described as follows:

$$J_{\text{aug}} = \begin{pmatrix} f_x & f_y & 0 \\ g_x & g_y & g_{\alpha_{\text{select}}} \\ & e_k^T & \end{pmatrix}. \tag{22}$$

Assuming that α_{select} corresponds to bus i, the components of P and Q in $g_{\alpha\text{select}}$ can be expressed as follows: For bus i

$$g^P_{\alpha_{\text{select}},i} = P_{l0}\left(\frac{V}{V_0}\right)^{\alpha}\log\left(\frac{V}{V_0}\right) \tag{23a}$$

$$g^Q_{\alpha_{\text{select}},i} = Q_{l0}\left(\frac{V}{V_0}\right)^{\beta}\log\left(\frac{V}{V_0}\right)\frac{d\beta_i}{d\alpha_{\text{select}}}. \tag{23b}$$

For other buses (bus j) with dynamic loads

$$g^P_{\alpha_{\text{select}},j} = P_{l0}\left(\frac{V}{V_0}\right)^{\alpha}\log\left(\frac{V}{V_0}\right)\frac{d\alpha_j}{d\alpha_{\text{select}}} \tag{24a}$$

$$g^Q_{\alpha_{\text{select}},j} = Q_{l0}\left(\frac{V}{V_0}\right)^{\beta}\log\left(\frac{V}{V_0}\right)\frac{d\beta_j}{d\alpha_{\text{select}}}. \tag{24b}$$

In *Scenario Two*, if the load exponent is selected as the parameter, the tracing direction is not normal to the branch at the long-term SNB point [7], but it is normal to the branch at the SIB point [8]. If it is the former, the SNB point can be solved without much effort. However, if it is close to the latter, the continuation parameter should be changed from the system parameter to one of the state variables that experiences more change.

V. Consideration of Load Change With Respect to Time

In CQSS analysis, there is no time integration involved. However, the time information is indirectly obtained during the equilibrium tracing. This time information is based on internal delays of discrete controls. The transition time step $t_{k+1} - t_k$ is determined by the shortest internal delay or sampling period of the long-term components (z_D). More specifically, in this time step, z_D will be updated according to some control logic. The continuation method introduces parameter λ or α_{select} to easily trace the equilibrium of the system under the step-size control. During the process of the OLTC action, λ or α_{select} also varies according to its time characteristics. Take λ as the example. Its time function is indicated as $\lambda(t)$ in the CQSS simulation. An approach should be found to appropriately consider how λ changes in the determined time interval $t_{k+1} - t_k$, so as to meet its time function.

In the continuation method, the prediction and correction can be made, respectively, as follows:

$$(\bar{x}_{k+1}, \bar{y}_{k+1}, \bar{\lambda}_{k+1}) = (x_k, y_k, \lambda_k) + \sigma_k \cdot [dx \quad dy \quad d\lambda]^T \tag{25}$$

$$(x_{k+1}, y_{k+1}, \lambda_{k+1}) = (\bar{x}_{k+1}, \bar{y}_{k+1}, \bar{\lambda}_{k+1}) + [\Delta x \quad \Delta y \quad \Delta\lambda]^T. \tag{26}$$

TABLE I
Parameters of the Dynamic Loads in the Simulation (Scenario Two)

Real power	α_S	α_T	T_P
	0	2.0	200.0 [s]
Reactive Power	β_S	β_T	T_Q
	0	2.0	160.0 [s]

Thus, the equation for computing the step size is

$$\sigma_k = \frac{\lambda_{k+1} - \lambda_k - \Delta\lambda}{d\lambda}. \tag{27}$$

In (27), λ_{k+1} and λ_k should be known from its time function. Similarly, $\alpha_{\max,k+1}$ and $\alpha_{\max,k}$ could be obtained from (21). If λ is taken as the continuation parameter, then $\Delta\lambda$ will be equal to zero in the correction stage. Then the step size σ_k can be obtained as follows:

$$\sigma_k = (\lambda_{k+1} - \lambda_k)/d\lambda. \tag{28}$$

At each time step, this step size should be recalculated to fit the load variation in this period. It is noted that the Jacobian used in the corrector stage depends on the state variables from the predictor stage. However, in order to get $d\lambda$ and $\Delta\lambda$ for the computation of the step size, at first, the same Jacobian as in the predictor is also used in the corrector. After the approximate step size is obtained, we update the Jacobian in the corrector, get the new $\Delta\lambda$ by solving (10), and calculate the step size again by using (27). This procedure will be repeated until the error between the updated $\Delta\lambda$ and the old one is within some tolerance.

VI. Numerical Results

The modified WECC 179-bus system is employed here to demonstrate the efficacy of the proposed methodology for analysis of long-term voltage instability. The main features of modeling and modification of the system in this simulation are as follows.

- Each generator is represented with the two-axis dynamic model [11] at its equilibrium condition. It includes automatic voltage regulator (AVR), the speed governor, the field and armature current limits, as well as the real power generation limit.

For *Scenario One*

- Sixty OLTCs are equipped at selected load buses.
- Before full load recovery, all the loads at the distribution sides of the OLTCs are constant impedance.
- After complete restoration by the OLTCs, all loads are increased with constant MVA load assumption.
- Each OLTC has an operating range of 0.8-1.1; the step size of the tap ratio is set as 0.006 25.
- The system at the base case has a total load demand of 57 746 MW.

For *Scenario Two*

- All the loads at the distribution sides of the OLTCs are modeled as thermostatic loads, and the parameters of these loads in the simulation are shown in Table I.
- All the OLTCs are blocked at their initial tap ratios.

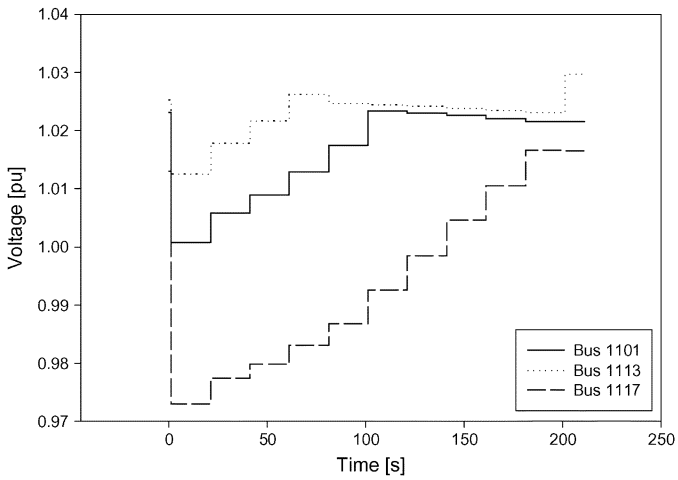

Fig. 4. Voltage change versus time during the load restoration.

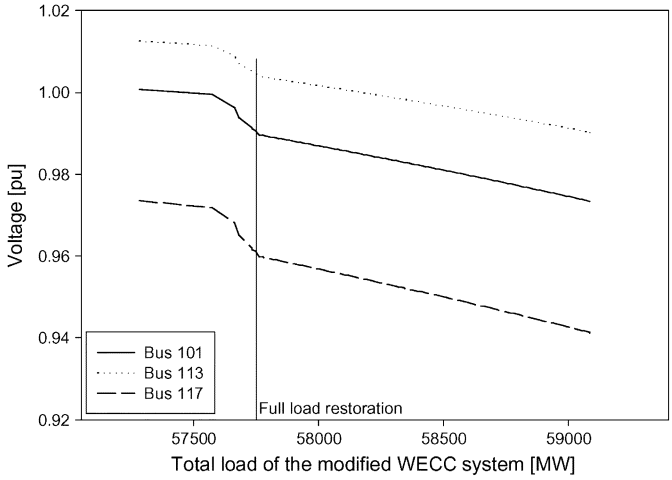

Fig. 5. PV diagram by using continuation-based QSS simulation.

A. CQSS Simulation for Scenario One

The contingency simulated for Scenario One in this case is an outage of the generating unit at bus 116. It is applied to the base case mentioned above. Due to the voltage dependent short-term load characteristic, the system total real power load is 57 283 MW right after the contingency. Hereafter, CQSS simulation will be adopted to obtain more information on the system voltage stability.

1) Step One (During the Load Restoration): In this step, only tap dynamics are considered for restoring the system load to the pre-contingency level. The OLTCs begin their actions 20 s after applying the contingency. The system real power load is recovered to about the initial load under pre-fault condition when $\mathrm{t} = 201$ s. The voltages at the distribution side buses of the OLTCs increase, whereas voltages at other buses decrease due to the load restoration. Fig. 4 shows the changes of voltages at buses 1101, 1113, and 1117 with respect to time. Note that these buses are selected from the distribution-side buses experiencing large voltage deviation after the contingency, and their high-voltage side buses are 101, 113, and 117, respectively.

2) Step Two (After the Complete Restoration): Once load restoration has been completely achieved, the system settles down to a stable long-term equilibrium. In order to evaluate proximity to voltage instability of the system, CQSS traces equilibrium curves with a given direction of load increase until the tangential component corresponding to load parameter changes its sign. For this process, all the loads are switched into constant power, and the speed of load increasing is taken into account. In this simulation, the real power load is assumed to be increased by 10 MW for each 10 s. By adjusting the step size in the application of the continuation method, CQSS can trace the system trajectory with the given load increasing speed until reaching the SNB point. When the generating unit at bus 46 hits its field current limit, the system finally collapses at $\mathrm{t} = 1445$ [s]. Using the CQSS, we can obtain the complete system PV curves as shown in Fig. 5.

In the predictor, null $d\lambda$ implies the singularity of J_{xy}. Table II shows the values of $d\lambda$ in the last five steps. For the system, the load parameter λ increases according to the step size after the complete restoration, until the SNB occurs at a load level of 59 083 MW, where a nearly zero $d\lambda$ is detected.

TABLE II
$d\lambda$ IN THE LAST FIVE STEPS

Time (s)	1416	1426	1436	1441	1445
$d\lambda$	0.004156	0.004044	0.003785	0.002870	-.0001965

The assumption of constant power in this technique may require caution in application due to the following two reasons: In simulation, first, one or more OLTCs can reach their limits, and the corresponding loads might not be fully restored. Second, the dead band effects in OLTCs' operation are not wholly taken into account in the applied technique with the constant power assumption. In these cases, the technique may give approximate results of active power margins. However, the objective of the technique is to provide proximity information to the long-term SNB point, and the concept of active power margin itself implies uncertainty by the direction of load increase. If active power margin with constant power assumption is not sufficient, for more accurate margin calculation, the precise margin-estimation method can be applied, which performs the gradual load increase without converting loads to constant power.

3) Verification of the Exponent-Based Load Restoration: This subsection considers the case in which the exponent-based dynamic load model is used instead of OLTCs for load restoration. In this simulation, that is, the OLTCs are blocked at their initial tap ratios, and the loads participating in load recovery in Scenario One are modeled with the exponent-based load restoration. This is for verification of the proposed model with the differential equation-based model. For this purpose, we developed the original QSS (OQSS) simulation tool, including the differential dynamic load model. Fig. 6 shows time versus voltage curves of buses 1101, 1113, and 1117 with CQSS and OQSS simulation. One can see that this simulation applies the contingency at 5 (s) and the simulation time reaches 1000 (s). From Fig. 6, the voltage magnitudes in CQSS simulation match closely those in OQSS simulation. Fig. 7 shows time versus real load restoration curves at bus 1117 with CQSS and OQSS. Load restoration with the exponent-based model is a little bit faster, and the largest mismatch between the two results during the simulation is about 3.09 MW.

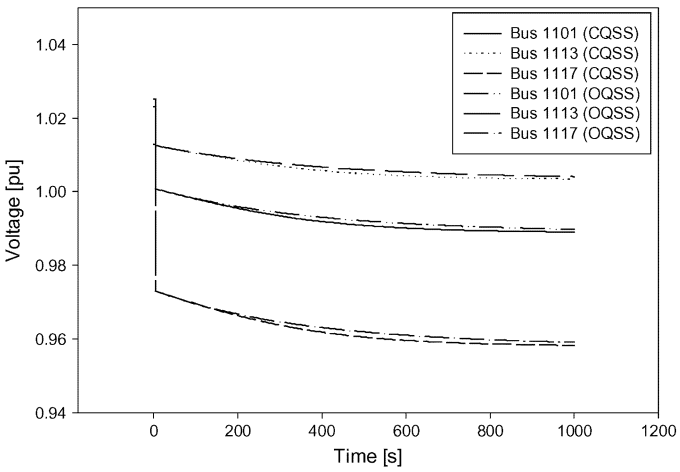

Fig. 6. Time versus voltage during load restoration with CQSS and OQSS.

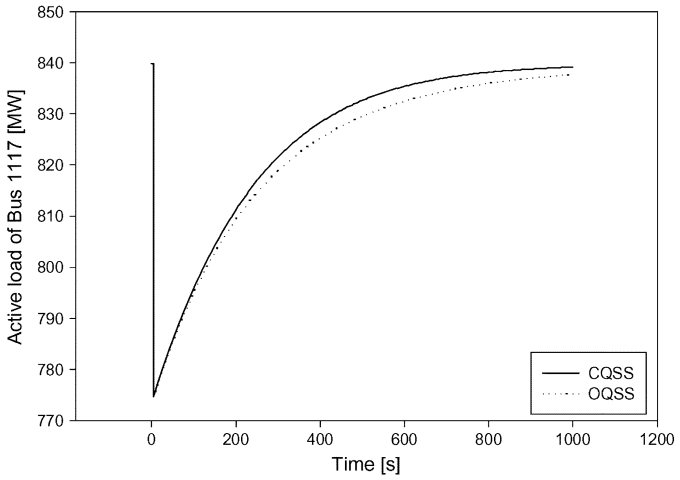

Fig. 7. Time versus real load restoration at bus 1117 with CQSS and OQSS.

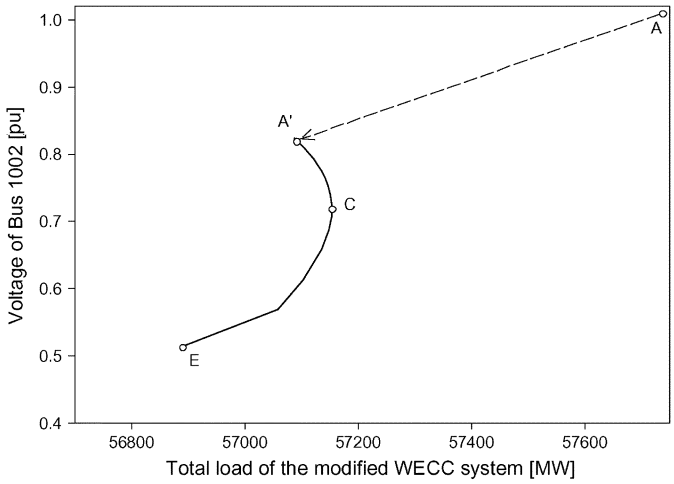

Fig. 8. Post-contingent PV curve of Bus 1002 (Scenario Two).

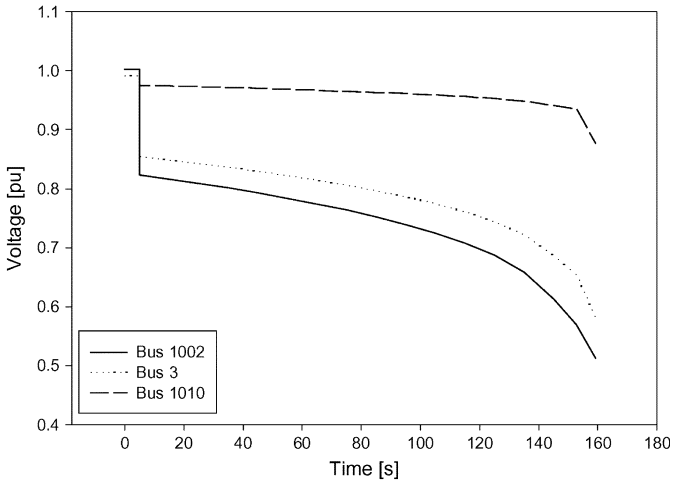

Fig. 9. Time versus voltage curves at buses 1002, 3, and 1010.

B. CQSS Simulation for Scenario Two

1) Simulation Results: The contingency considered for Scenario Two is tripping the generating unit at bus 4, and the load level is the same as before. The outage has been applied at $\mathrm{t} = 5$ (s). After the contingency, CQSS is applied for long-term voltage stability analysis. In this simulation, only thermostatic load self-restoration is considered in order to mainly illustrate the effect of applying the continuation method in CQSS. The outage leads to the system voltage collapse due to the SIB point. During this process, the generating units at buses 9 and 18 hit their field current limits. Also the system crosses the long-term SNB point during the tracing.

Fig. 8 shows the post-contingency PV curve of bus 1002. In the figure, A' is the system operating point just after the contingency, where $P_{A'} = 57\,088$ MW. In Fig. 8, E corresponds to the SIB point. C represents the turning point of the PV curve, and the real power at this point is around 57 153 MW. Fig. 9 shows the time evolution of voltages of buses 1002, 3, and 1010 in the system. Buses 1002 and 1010 are distribution-side buses of buses 2 and 10, respectively.

In the simulation, the generator of bus 9 hits its field current limit at 152.84 [s], and generator 18 reaches its limit around the SIB point. CQSS stops after passing the SIB point (E). The SIB point can be readily identified by the null $d\alpha_{\mathrm{select}}$ in the tangent vector. Table III shows how the continuation parameter α_{select} changes in the last five steps and the corresponding time.

TABLE III
$d\alpha$ IN THE LAST FIVE STEPS

TIME(S)	125	135	145	152.84	159.15
αSELECT	-0.63627	-0.50171	-0.27489	-0.12353	0.11038

2) Computational Aspects: In this subsection, some computational advantages of CQSS are discussed. First, CQSS uses the continuation method to trace short-term equilibrium trajectories with respect to evolution of long-term dynamics in the systems, so near the SIB point, it can remove singularity of the short-term Jacobian, whereas the original QSS program diverges near this point. Fig. 10 plots time versus voltage of bus 1002 from the simulation of CQSS and OQSS when time step is set to 10 (s). After applying the contingency, OQSS diverges at the 15th step because it faces the problem of numerical singularity. CQSS, however, traces further and shows the robust convergence characteristic with adaptive switching continuation parameter from α_{select} to one of other state variables to remove the singularity.

Second, the predictor step in CQSS can reduce N-R iterations in the corrector. As mentioned earlier, the predictor takes

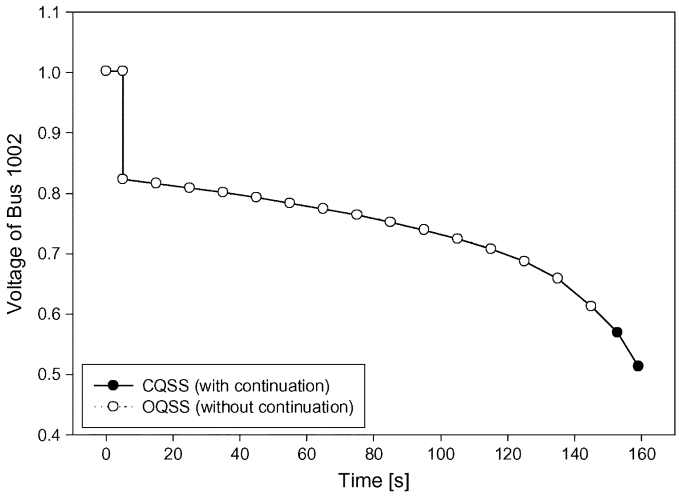

Fig. 10. Time versus voltage curves with CQSS and OQSS

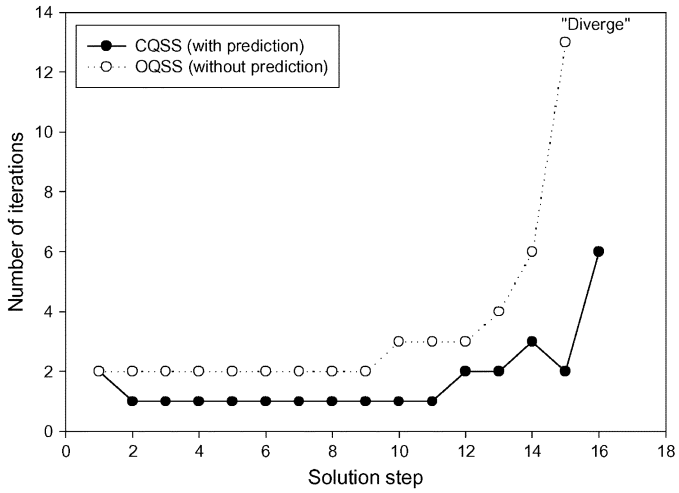

Fig. 11. Iteration numbers in correction phase with and without prediction.

one N-R iteration to get the tangent vector at the current solution. Fig. 11 compares the iteration numbers in CQSS and OCSS simulation. From steps 2–9, the simulation with CQSS demands one iteration less than that of OQSS. Then, from steps 10–14, as the trajectory approaches closer to the SIB point, the short-term solution without prediction requires about two times more iterations than that of OQSS. Around the SIB point, OQSS diverges at step 15 after performing 13 iterations; however, CQSS is numerically well conditioned in the whole simulation. In CQSS, the predictor also has an important role for convergence of solutions due to the fact that without prediction, it may fail to converge when the continuation parameter is changed near the point.

From the tangent vector in the predictor, in addition, we can get valuable information for checking singularity of the Jacobian (J_{xy}) without any more calculation. For this purpose, OQSS needs a subroutine for the sensitivity of the total reactive power generation, and it demands one N-R iteration to inverse the Jacobian. Thus, if singularity checking is required in OQSS, there is little difference between CQSS and OQSS, from the viewpoint of computation burden. From Fig. 11, up to step 14, the sum of iterations in CQSS simulation is 19, and that in OQSS simulation is 37. When only considering these iteration numbers, application of continuation can reduce about 48% of computational cost. However, factorization of the Jacobian is performed once in a correction phase; thus, in the our experience, CQSS takes around 25% less computation than OQSS for *Scenario Two*.

C. Discussion

In *Scenario Two*, QSS analysis incorporates the load self-restoration, which is represented by the differential equations associated with z_C in the long-term time scale. In CQSS simulation, a new way is proposed to consider the load restoration by introducing the continuation method. It parameterizes and varies the load exponent instead of integrating the dynamic load model in the simulation. Usage of the load-exponent-based model does not require large implementation burden due to the fact that the original model is simple. In addition, CQSS applies the locally parameterized continuation method to remove the numerical difficulty around the SIB point. For this application, CQSS needs a slightly complicated algorithm for continuation parameter selection, but this process gives an advantage of robust QSS simulation.

In *Scenario One*, QSS simulation is very fast if one avoids refreshing the Jacobian matrix. However, the Jacobian has to be updated when some of the devices are hitting their limits. Although CQSS involves two Jacobian matrices in the predictor and the corrector, they could be the same for fast computation. Furthermore, the predictor is much less computationally demanding than the corrector. For the predictor, we have to solve (9) only once. The corrector needs an iterative solution similar to solving the equations in the original QSS simulation. Thus, the simulation time in CQSS is almost the same as QSS under light load conditions. When the system approaches the SIB point, the Newton method for the original QSS becomes ill conditioned due to singularity of the Jacobian. The Newton method often takes longer time for a solution or fails to converge before the Jacobian matrix actually becomes singular. At the SIB point, the Newton method is divergent and a unique solution for state variables could not be found, so the original QSS simulation might take longer time than the CQSS under heavy load conditions.

Similar conclusions apply for *Scenario Two* around the SIB point. As mentioned before, the SIB of long-term dynamics corresponds to a singular J_{xy}. CQSS can solve the short-term equilibrium near at the singular point because adequate selection of the continuation parameter avoids the ill-conditioned Jacobian matrix from the short-term dynamics and algebraic equations.

VII. Conclusion

In this paper, QSS simulation combined with the continuation method is developed. Compared to the original QSS analysis, the CQSS is numerically well conditioned by introducing the continuation parameter. It can also readily identify the SIR in the long-term time scale. Furthermore, the combined effects of the OLTCs and the load change on voltage stability can be taken into account. Parameterization of the load exponents through continuation method provides another approach to approximate the

load self-restoration procedure. CQSS presents a robust simulation for long-term voltage stability analysis while retaining the realistic ingredients needed to reproduce voltage phenomena: voltage dependence of the load and effects of the OLTC discrete control.

REFERENCES

[1] C. Taylor, *Power System Voltage Stability*, ser. EPRI Power System Engineering. New York: McGraw-Hill, 1994.

[2] T. Van Cutsem and C. Vournas, *Voltage Stability of Electric Power Systems*. Norwell, MA: Kluwer, 1998.

[3] *Voltage Stability Assessment: Concepts, Practices and Tools*: IEEE PES Power System Stability Subcommittee, 2002. IEEE Product no. SP101PSS.

[4] P. Kundur, J. Paserba, V. Ajjarapu, G. Andersson, A. Bose, C. Canizres, N. Hatziargyriou, D. Hill, A. Stankovic, C. Taylor, T. Van Cutsem, and V. Vittal, "Definition and classification of power system stability," *IEEE Trans. Power Syst.*, vol. 19, no. 2, pp. 1387–1401, May 2004.

[5] T. Van Cutsem, Y. Jacquemart, J. Marquet, and P. Pruvot, "A comprehensive analysis of mid-term voltage stability," *IEEE Trans. Power Syst.*, vol. 10, no. 2, pp. 1173–1182, May 1995.

[6] D. Karlsson and D. J. Hill, "Modeling and identification of nonlinear dynamic loads in power systems," *IEEE Trans. Power Syst.*, vol. 9, no. 1, pp. 157–166, Feb. 1994.

[7] T. Van Cutsem and C. Vournas, "Voltage stability analysis in transient and mid-term time scales," *IEEE Trans. Power Syst.*, vol. 11, no. 1, pp. 146–154, Feb. 1996.

[8] V. Venkatasubramanian, H. Schattler, and J. Zaborszky, "A taxonomy of the dynamics of the large power system with emphasis on its voltage stability," in *Proc. Int.Work. Bulk Power System Voltage Phenomena II—Voltage Stability and Security*, 1991, pp. 9–44.

[9] Z. Feng, V. Ajjarapu, and Bo. Long, "Identification of voltage collapse through direct equilibrium tracing," *IEEE Trans. Power Syst.*, vol. 15, no. 1, pp. 342–349, Feb. 2000.

[10] V. Ajjarapu and C. Christy, "The continuation power flow: A tool for steady state voltage stability analysis," *IEEE Trans. Power Syst.*, vol. 7, no. 1, pp. 416–423, Feb. 1992.

[11] D. J. Hill, "Nonlinear dynamic load models with recovery for voltage stability studies," *IEEE Trans. Power Syst.*, vol. 8, no. 1, pp. 166–172, Feb. 1993.

[12] Q. Wang and V. Ajjarapu, "A novel approach to implement generic load restoration in continuation-based quasisteady-state analysis," *IEEE Trans. Power Syst.*, vol. 20, no. 1, pp. 516–518, Feb. 2005.

Qin Wang (M'02) received the Ph.D. degree in electrical engineering from Iowa State University, Ames, in 2001.

Currently, she is a Hardware Engineer with EMC Corporation, Hopkinton, MA. Her current research interests mainly include power system stability analysis and simulation as well as power electronics application.

Hwachang Song (S'00–M'03) received the B.S., M.S., and Ph.D. degrees in electrical engineering from Korea University, Seoul, Korea, in 1997, 1999, and 2003, respectively.

He was a Postdoctoral Visiting Scholar at Iowa State University, Ames, and a Researcher with the Advanced Power Systems Research Center, Korea University, from 2003 to 2004. Currently, he is a Lecturer in the School of Electronic and Information Engineering, Kunsan National University, Jeonbuk, Korea. His interests include optimization, system protection schemes, and FACTS equipment.

Venkataramana Ajjarapu (S'86–M'86–SM'91) received the Ph.D. degree in electrical engineering from the University of Waterloo, Waterloo, ON, Canada, in 1986.

Currently, he is an Associate Professor in the Department of Electrical Engineering and Computer Engineering, Iowa State University, Ames.